PHYSICAL REVIEW C VOLUME 8, NUMBER 6 DECEMBER 1973

Gamma-Ray-Multiplicity Measurements for (α, p), (α, α'), (d, α), (p, α), (d, p), and (p, p') Reactions*

J. H. Degnan,† B. L. Cohen, G. R. Rao, K. C. Chan, and L. Shabason
Nuclear Physics Laboratory, University of Pittsburgh, Pittsburgh, Pennsylvania 15260
(Received 8 June 1973)

Using a method introduced previously measurements were made of the γ-ray multiplicity N_γ (the average number of γ rays emitted in the decay of residual nuclei left by nuclear reactions) as a function of excitation energy E^* for (p,α) and (d,α) reactions on ^{51}V, ^{56}Fe, and ^{57}Fe targets; (α,p) reactions on ^{51}V, ^{56}Fe, ^{57}Fe, ^{58}Ni, ^{64}Ni, ^{93}Nb, and Ag; (α,α') reactions on ^{51}V, ^{55}Mn, ^{56}Fe, ^{57}Fe, ^{59}Co, and ^{64}Ni; (d,p) reactions on ^{51}V, ^{55}Mn, ^{56}Fe, Ag, and ^{119}Sn; and (p,p') reactions on ^{56}Fe, ^{112}Sn, and ^{122}Sn. Bombarding energies ranged from 12 to 19 MeV. N_γ was observed to be generally between 1 and 5 for E^* between 3 and 10 MeV for the (p,p'), (d,p), (d,α), (p,α), and (α,α') reactions investigated, and somewhat higher for the (α,p) reactions. N_γ increases with E^*, and is larger for higher angular momentum transfer reactions although it is not as much larger as angular momentum transfer considerations alone would suggest. (This can be explained as a level-density effect for compound-nucleus reactions—the average angular momentum of the states excited by the reactions is severely limited by the level-density spin-cutoff parameter.) The dependence of N_γ on the average excess angular momentum of the residual nuclei was investigated using calculated spin distributions for the residual nuclei. This dependence is similar to that for neutron capture N_γ's—N_γ increases with excess angular momenta for excess angular momenta of more than 2 or 3 units.

I. INTRODUCTION

This paper reports measurements of the γ-ray multiplicity N_γ (the average number of prompt γ rays emitted in the decay of residual nuclei left by specific nuclear reactions) for some 30 reactions—(α,α'), (α,p), (p,α), (d,α), (p,p'), and (d,p) reactions on various targets—as a function of residual-nucleus excitation energy. These results together with the results for some 26 reactions—(p,p') and (d,p)—reported previously by these authors[1,2] are compared in an attempt to find systematic differences in N_γ for different reactions, and in particular, to investigate the dependence of N_γ on the excess angular momentum of the residual nucleus. The results are also compared to the neutron-capture γ-ray multiplicities measured by Muelhause[3] and by Draper and Springer.[4]

Work by other authors on this topic includes measurements of N_γ for neutron capture,[3,4] for fission,[5,6] and for ^{12}C and α capture.[7] In Ref. 3, N_γ was measured for thermal neutron capture using coincidence and singles detection of γ rays with NaI scintillation detectors, and assuming that the γ-detection efficiency is independent of γ energy for the energy range of interest. In Ref. 4, N_γ was measured for resonance neutron capture using a 10.2-cm-thick NaI detector, assuming a constant γ-detection efficiency, and using the ^{10}B(n,γ) reaction as a calibration standard since N_γ is known for that reaction.[4] In Ref. 5, prompt γ rays from thermal ^{235}U(n,f) were detected in coincidence with fission fragments and the total number and energy of γ rays emitted per fission was determined as a function of fission-fragment mass. In Ref. 6, prompt γ rays from thermal ^{235}U(n,f), ^{239}Pu(n,f), and spontaneous fission of ^{252}Cf were detected in coincidence with fission fragments and N_γ per fission was determined as a function of γ energy. In Refs. 5 and 6, γ rays were distinguished from neutrons by time-of-flight techniques, and γ rays were detected with NaI scintillators. Response matrix methods were used to account for the energy dependence of the γ detection efficiency and for the pulse-height response. In Refs. 5 and 6, the average N_γ for all excitation energies of the fission products was determined. In Ref. 7, N_γ was determined for ^{12}C and α capture as a function of bombarding energy, using detection of γ rays in coincidence with the incident beam and in anticoincidence with the transmitted and scattered beam (for scattering angles up to 75°). The excitation energies of the first compound nucleus ranged from 25 to 100 MeV in the cases reported, and no distinction of the different particle-emission modes was made in determining the average N_γ.

For lower residual-nucleus excitation energies, N_γ may be deduced from level schemes.[1,8]

Work reported in the literature which is related to γ-ray multiplicity includes that of Coceva,

Corvi, and Giacobbe[9] and of Stolovy *et al.*[10] in which the spins of neutron-capture resonances are determined by a measured quantity which is closely related to the γ-ray multiplicity—the ratio of singles- to coincidence-γ-detection rates with a low coincidence-detection threshold and a high singles-detection threshold. Reference 9 also discusses a technique for calculating the average N_γ for a given initial spin and excitation energy. The work of Huizenga and Vandenbosch[11] on isomer ratios relates isomer to ground-state production ratios to the γ-ray multiplicity and the level-density spin-cutoff parameter σ.

The work reported here employs the technique introduced in Ref. 1, which will be briefly described in the next section.

II. EXPERIMENTAL SETUP AND DATA ANALYSIS

A self-supporting foil target is bombarded with a monoergic beam of particles, and emitted charged particles and γ rays are detected in coincidence. The γ rays are detected with a plastic scintillation detector (8.9-cm-diam × 1.9-cm-thick Pilot B scintillator mounted on a 12.7-cm RCA C70133B 14-stage photomultiplier) and identified by their time of flight. With a γ-ray detection threshold of 120 keV, the efficiency for detecting γ rays was calculated and checked experimentally; it is well approximated in the energy region 0.4 to 6 MeV by

$$\epsilon_{\gamma i} = a - bE_{\gamma i}\,, \tag{1}$$

where $\epsilon_{\gamma i}$ is the efficiency for detecting the ith γ ray, $E_{\gamma i}$ is the energy of the ith γ ray, and a and b are parameters.[1] N_γ is given by[1]

$$N_\gamma = \frac{1}{a}\left(\frac{4\pi}{\Omega}\frac{N_g}{N_p} + bE^*\right)\,, \tag{2}$$

where Ω is the solid angle of the scintillation detector, N_g/N_p is the ratio of γ rays detected in coincidence with charged particles to charged particles detected, and E^* is the excitation energy of the residual nucleus. E^* is readily obtained from the energy of the particle detected in coincidence. N_γ and N_g/N_p are, of course, functions of E^*. Equation (2) is obtained by substituting Eq. (1) into

$$N_g/N_p = \frac{\Omega}{4\pi}\sum_{i=1}^{N_\gamma}\epsilon_{\gamma i}$$

as further described in Ref. 1.

III. THEORETICAL CONSIDERATIONS

It is reasonable to expect that N_γ depends on the initial excitation energy, the initial spin distribution and ground-state spin (i.e., the excess angular momentum which must be disposed of by γ-ray emission in the deexcitation process), and on the level structure of the decaying nucleus. In fact, a procedure for calculating N_γ which uses known level schemes and branching ratios and theoretical transition rates and level densities for higher excitation energies is discussed in Ref. 9. Both complicated calculations[9] and simpler considerations indicate some general trends to be expected for N_γ. Some pertinent remarks on this are listed below for later reference:

(1) N_γ is expected to increase with residual-nucleus excitation energy E^*. Neutron capture N_γ's[3,4] (for which E^* is the neutron binding energy of the product nucleus) are typically 2.5 to 4, whereas for excitation to the first excited state, N_γ is no more than 1. The results in Refs. 1 and 2 support this.

(2) N_γ should increase with the excess angular momentum which must be disposed of in the deexcitation γ-ray cascades. This is a consequence of the fact that $E1$, $E2$, and $M1$ transitions predominate, so that each step in the deexcitation cascade can dispose of 1 or at most 2 units of excess angular momenta. Thus N_γ should depend on the probability distribution $f(I)$ of the angular momentum I excited by the reaction. If we define $\bar{I}$ as the average angular momentum of the residual nucleus[12] at excitation energy E^*, and I_R as the ground-state spin of the residual nucleus, one would expect N_γ to increase as $|\bar{I} - I_R|$ increases (for the same E^*).

(3) Since the average angular momentum of states available for excitation (at a given excitation energy) increases with target-nucleus mass A, and since angular momentum barriers decrease with increasing A, one might expect that for any given reaction mechanism, $\bar{I}$ and hence N_γ should be larger for higher-A target nuclei than for lower-A target nuclei.

(4) Odd-A and odd-odd nuclei have low-energy states and isomeric states with high angular momenta. El and Ml transitions are not prompt for $l > 2$, and the experimental method used here detects only prompt γ rays with energies above a few hundred keV, so it should be expected that reactions leaving an odd-A or odd-odd final nucleus have a lower "measured" N_γ than similar reactions leaving an even-even final nucleus.

(5) One might expect that $|\bar{I} - I_R|$ and hence N_γ would be higher than usual for a given type of reaction and E^* if the spin of the target nucleus is high while the ground-state spin of the product nucleus is low. Calculations of $f(I)$ for compound nucleus (CN) reactions indicate that this target-spin–product-spin effect is present but small for

the cases studied (cf. Fig. 9). This effect is certainly present, at least on $|\bar{I} - I_R|$, for thermal and resonant neutron capture, since I is $I_T \pm \frac{1}{2}$, where I_T is the target spin.

(6) $f(I)$ is calculable for (d,p) reactions[13] as described in Appendix I. It involves the use of distorted-wave Born-approximation (DWBA) (d,p) cross sections and spectroscopic strengths. Because low angular momentum transfers are kinematically favored in (d,p) reactions, $\bar{I}$ for zero-spin targets turns out to be typically about 2.

(7) $f(I)$ is calculable for CN reactions,[13-15] assuming the statistical theory of nuclear reactions is valid. The calculations, described in Appendix I, involve sums over terms which are products of transmission coefficients (barrier penetrabilities) for the incident and emitted particles and the spin part of the level density. The limits of the sums are determined by angular momentum selection rules. The resulting spin distributions yield $\bar{I}$'s close to the level-density spin-cutoff parameter σ for a large variety of reactions. Calculated spin distributions and $\bar{I}$'s are shown in Fig. 7 in the next section.

IV. RESULTS AND DISCUSSION

Determinations of N_γ vs E^* are shown for 30 reactions (not reported previously) in Figs. 1 and

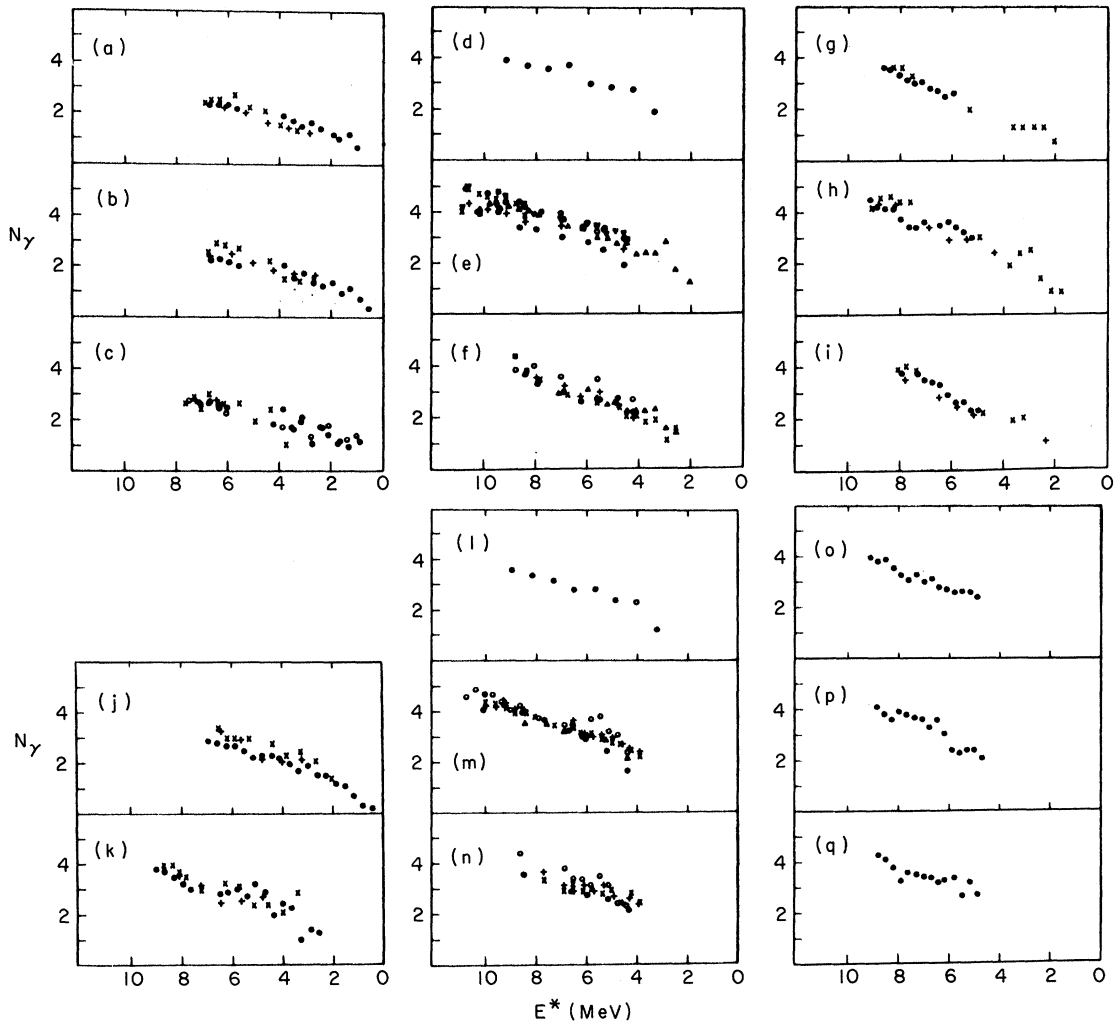

FIG. 1. γ-ray multiplicity measurements: (a) $^{51}V(d,p)$, $E_0=12$ MeV; (b) $^{55}Mn(d,p)$, $E_0=12$ MeV; (c) $^{56}Fe(d,p)$, $E_0=12$ MeV; (d) $^{56}Fe(p,p')$, $E_0=15$ MeV, $\theta_p=90°$; (e) $^{112}Sn(p,p')$, $E_0=15$ MeV, $\theta_p=90°$; (f) $^{122}Sn(p,p')$, $E_0=15$ MeV, $\theta_p=90°$; (g) $^{51}V(\alpha,\alpha')$, $E_0=18,19$ MeV; (h) $^{56}Fe(\alpha,\alpha')$, $E_0=18,19$ MeV; (i) $^{57}Fe(\alpha,\alpha')$, $E_0=18,19$ MeV; (j) $Ag(d,p)$, $E_0=12$ MeV; (k) $^{119}Sn(d,p)$, $E_0=12$ MeV; (l) $^{56}Fe(p,p')$, $E_0=15$ MeV, $\theta_p=130°$; (m) $^{112}Sn(p,p')$, $E_0=13$ MeV, $\theta_p=130°$; (n) $^{122}Sn(p,p')$, $E_0=15$ MeV, $\theta_p=130°$; (o) $^{55}Mn(\alpha,\alpha')$, $E_0=19$ MeV; (p) $^{59}Co(\alpha,\alpha')$, $E_0=19$ MeV; (q) $^{64}Ni(\alpha,\alpha')$, $E_0=19$ MeV. E_0 is the bombarding energy.

2. The different symbols represent different data runs. Gaps in the data are due to target impurities. An indication of the reliability of the data is given by its reproducibility. For the 10 cases for which only a single data run was made, this reliability was indirectly checked by the reproducibility of data for other cases run on the same experiment days.

N_γ increases with E^*, as expected and as noted previously.[1,2] The observed values of N_γ at higher E^* are similar to the neutron-capture γ-ray multiplicities reported in Refs. 3 and 4. A comparison of the frequencies of occurrence of N_γ for the neutron-capture cases reported in Refs. 3 and 4, and for the cases reported in this work (and in Refs. 1 and 2) is shown in Fig. 3. In Fig. 3, the N_γ's from this work are for E^* equal to the average neutron binding energy $\bar{B}_n$ for the neutron-capture cases.

In order to readily discern systematics of N_γ for nuclear reactions, smooth lines drawn through the data reported in this work and in Refs. 1 and 2 are plotted for different reactions on the same targets in Fig. 4, for the same reactions on different targets in Fig. 5, and for (p, p') reactions with two different particle-emission angles, 90

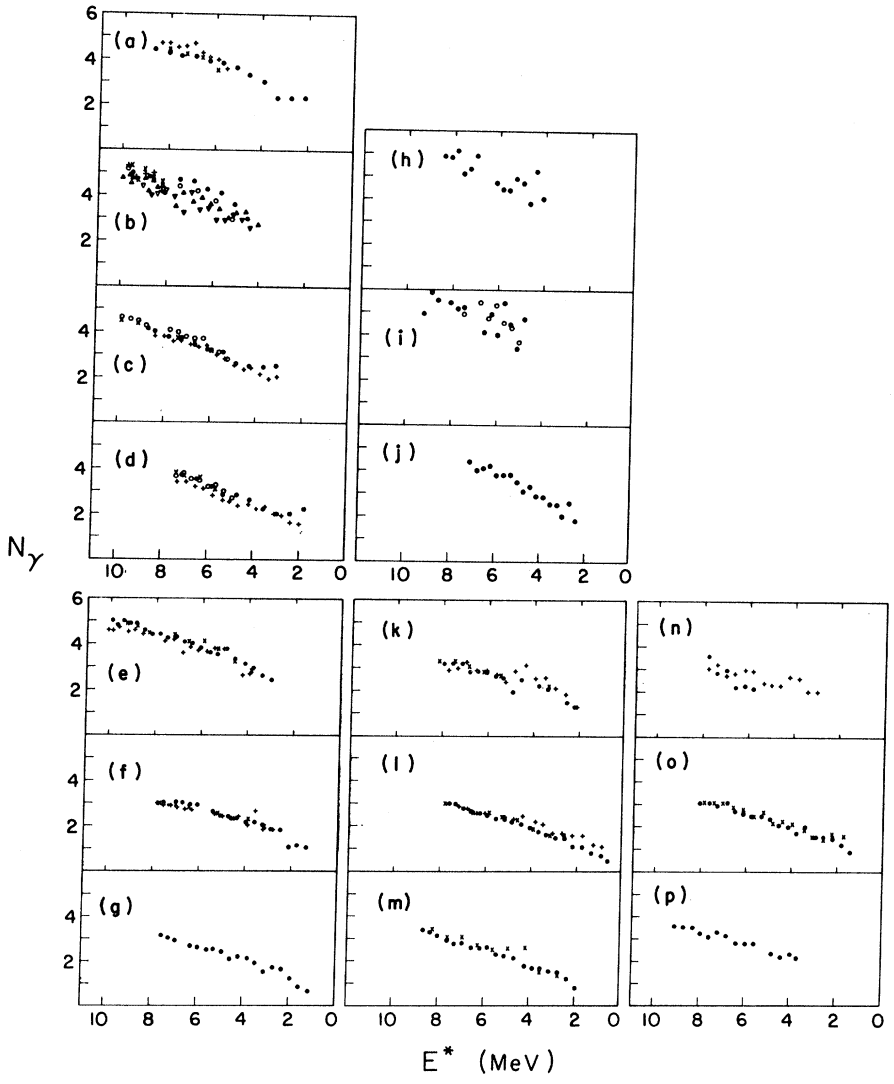

FIG. 2. γ-ray multiplicity measurements: (a) ^{58}Ni(α,p), E_0=18,19 MeV; (b) ^{51}V(α,p), E_0=18,19 MeV; (c) ^{56}Fe(α,p), E_0=18,19 MeV; (d) ^{57}Fe(α,p), E_0=18,19 MeV; (e) ^{51}V(p,α), E_0=17 MeV; (f) ^{56}Fe(p,α), E_0=17 MeV; (g) ^{57}Fe(p,α), E_0=17 MeV; (h) ^{93}Nb(α,p), E_0=19 MeV; (i) Ag(α,p), E_0=19 MeV; (j) ^{64}Ni(α,p), E_0=19 MeV; (k) ^{51}V(d,α), E_0=12 MeV; (l) ^{56}Fe(d,α), E_0=12 MeV; (m) ^{57}Fe(d,α), E_0=12 MeV; (n) ^{51}V(d,α), E_0=17 MeV; (o) ^{56}Fe(d,α), E_0=17 MeV; (p) ^{57}Fe(d,α), E_0=17 MeV. E_0 is the bombarding energy.

and 130°, in Fig. 6.

As can be seen in Fig. 6, the effects on N_γ in changing the lab scattering angle θ_p from 90 to 130° are small, if any, for (p,p') reactions on ^{56}Fe, ^{112}Sn, and ^{122}Sn (15-MeV bombarding energy). There is essentially no detectable effect for ^{112}Sn and ^{122}Sn. As for the slight decrease of N_γ for ^{56}Fe (p,p'), one should bear in mind that only one data run was made for ^{56}Fe (p,p') at each angle.

In order to facilitate interpretation of the results in light of the theoretical considerations of the previous section, calculated spin distributions for the residual nuclei for 10 different reactions (7 of them at 2 excitation energies) are shown in Fig. 7. For all the cases except for the (d,p) reactions, the calculations were done assuming a CN reaction mechanism. The ^{58}Ni and ^{112}Sn(p,p') reactions are known to be predominantly CN for the higher excitation energies studied here.[16] The emitted-particle energy spectra for the (p,α), (d,α), and (α,p) reactions have the evaporation

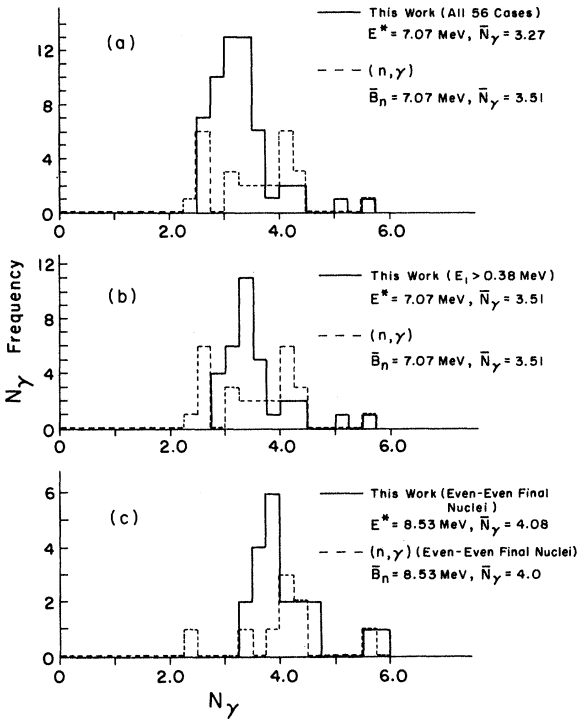

FIG. 3. Frequencies of occurrence of N_γ for reactions studied in this work (solid lines) and for neutron-capture cases (Refs. 3 and 4) (dashed lines). Part (a) shows N_γ for all cases investigated in this work and in Refs. 3 and 4. Part (b) shows only those cases from this work for which low-energy γ rays are not expected to be important (plus all the cases reported in Refs. 3 and 4). Part (c) shows only cases for which the product nuclei are even even. E_1 in part (b) is the energy of the first excited state of the product nucleus.

shape characteristic of CN reactions (cf. Fig. 8), and (α,p) reactions on ^{51}V, ^{56}Fe, ^{59}Co, ^{58}Ni, ^{62}Ni, and Cu reportedly[17,18] have isotropic angular distributions for bombarding energies less than 20 MeV, also characteristic of CN reactions. For higher bombarding energies, (α,p) reactions have forward-peaked angular distributions,[19] and, even for bombarding energies where the angular distribution is isotropic, there appears to be an anomalous dependence of the level-density parameter a, as determined by assuming a CN reaction mechanism, on bombarding energy,[19] so the assumption that the (α,p) reactions studied in this work are CN may be only partially correct. (α,α') reactions may have important direct reaction (DR) contributions, but the calculated spin distributions assuming a CN mechanism are still instructive for comparing α-induced with proton- and deuteron-induced spin distributions, assuming a CN mechanism for the α-induced reactions.

The most important feature of the calculated spin distributions for CN reactions is the strong dependence of $f(I)$ (and $\bar{I}$) on the level-density spin-cutoff parameter σ (for the residual nucleus). Even for reactions where excitation of higher angular momentum states is possible (for example, α-induced reactions), the peak of the spin distribution and the mean angular momentum $\bar{I}$ of the residual nucleus is not very different from the value of σ. This is because $f(I)$ is proportional to the spin part of the level density, $\rho(I)$, as discussed in Appendix I. The strong dependence of $f(I)$ on σ is illustrated in Fig. 9, parts (a) and (c). As can be seen in part (c), the relative probability for exciting states is strongly influenced by the angular momentum distribution of the states available for excitation—if $\rho(I)$ were a constant, the angular momentum for which $f(I)$ is maximum, I_m, would be over twice as large for the (α,p) reaction as for the (p,p') reaction. Since $\rho(I)$ is not constant but peaks near $I=\sigma$ (cf. Appendix I), I_m is not as much larger as angular momentum transfer considerations alone would imply.

In comparing N_γ for different reactions on the same target (cf. Fig. 4), the following remarks may be made:

(a) The biggest effect observed is that N_γ is considerably larger for the (α,p) reactions than for the (d,p) reactions (both reactions were studied for targets ^{51}V, ^{56}Fe, and Ag). This can be understood in terms of $\bar{I}$ [which is considerably larger for the (α,p) than for the (d,p) reactions as shown in Fig. 7] as discussed in remark (2) of the last section.

(b) N_γ is somewhat larger for ^{64}Ni(α,p) than for ^{64}Ni(p,p'), and it is about the same for ^{56}Fe(α,p) and ^{56}Fe(p,p') reactions. The fact that N_γ is not

much larger for the (α, p) reactions than for the (p, p') reactions, despite the higher angular momentum transfer of the (α, p) reactions, can be explained by the strong dependence of $\bar{I}$ on σ, as discussed earlier in this section and illustrated in Fig. 9. Since σ is not very different for the residual nuclei left by the (α, p) and (p, p') reactions, $\bar{I}$ is not very different, so, according to remark (2) of the last section, N_γ will not be very different. [While the relation between $\bar{I}$ and σ has been investigated only for CN reactions, and ^{64}Ni(p, p') is DR,[2,16] N_γ for ^{64}Ni(p, p') is the same[2] as for ^{60}Ni(p, p'), which is a predominantly CN reaction.[16]]

In addition to the aforementioned arguments, the residual nuclei for the (p, p') reactions are even-even, while those for the (α, p) reactions are odd A, which will superimpose an odd-even effect tending to decrease the measured N_γ for the (α, p) reactions.

(c) N_γ is somewhat larger for the (α, p) reactions than for the (α, α') reactions on targets ^{51}V, ^{57}Fe, and ^{64}Ni while it is about the same for both reactions on ^{56}Fe. While the size of N_γ for (α, p) reactions is qualitatively understood in terms of $\bar{I}$ [particularly insofar as it is not as much larger than N_γ for (p, p') reactions as angular momentum transfer considerations alone would imply], it is more difficult to explain for (α, α') reactions, which may have considerable DR contributions (for which $\bar{I}$ is not calculable at present). It is interesting to note that the size of N_γ indicates that $\bar{I}$ for (α, α') reactions is close to that calculated for a CN reaction mechanism.

(d) N_γ is smaller for the (d, p) reactions than for the (p, p') reactions studied on targets ^{56}Fe, ^{59}Co, and ^{60}Ni, but it is larger for targets ^{61}Ni, ^{103}Rh, and ^{117}Sn. N_γ is the same for the $^{120-122}$Sn(d, p) and (p, p') reactions studied. Except for the ^{103}Rh results, this might be explained by the odd-even effects discussed in remark (4) of the last section.

(e) N_γ is smaller for ^{56}Fe(p, α) than for ^{56}Fe(p, p'); this might also be an odd-even effect.

(f) No bombarding energy dependences of N_γ were found for the (d, α) and (p, α) reactions studied except for a small one in ^{116}Cd(p, p')—which was reported and discussed in Ref. 2.

In comparing N_γ for the same reactions on different targets (cf. Fig. 5) it is observed that

(a) The odd-even effects discussed in remark (4) of the last section seem to be present in the (α, p), (p, α), and (d, p) reactions studied, but not in the

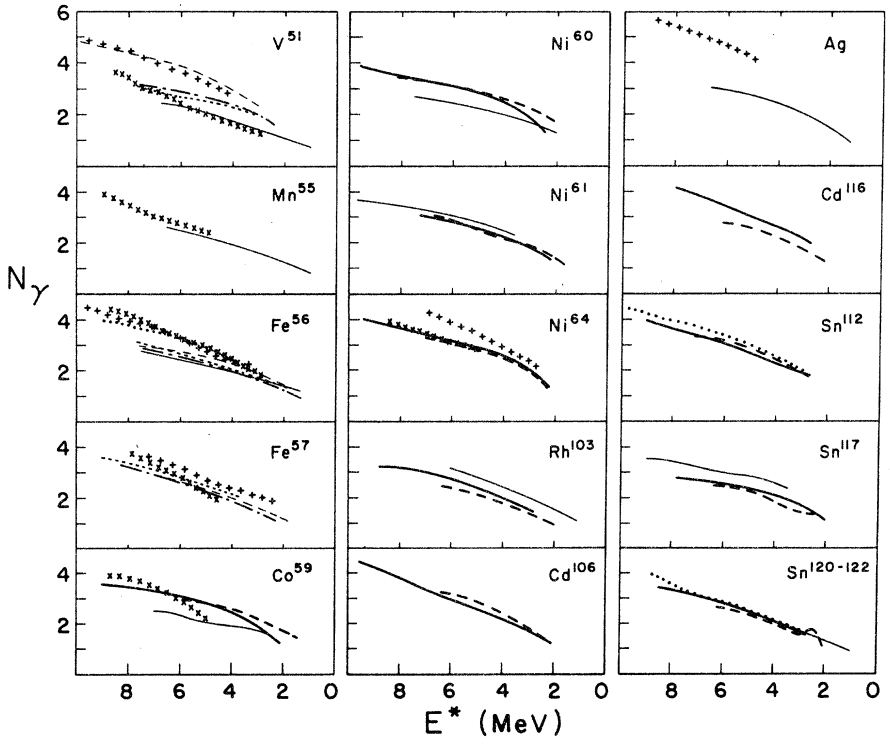

FIG. 4. Comparisons of N_γ for different reactions on the same targets. Symbols are as follows: – – –, (p,p'), E_0=12 MeV; . . . , (p,p'), E_0=15 MeV; ——, (p,p'), E_0=17 MeV; ——, (d,p), E_0=12 MeV; – – –, (p,α), E_0=17 MeV; — - —, (d,α), E_0=12 MeV; ---, (d,α), E_0=17 MeV; ×××, (α,α'), E_0=18,19 MeV; +++, (α,p), E_0=18,19 MeV.

(p, p') reactions studied.

(b) N_γ increases with A, as expected [discussed in remark (3) of the last section] for the (d, p) and (α, p) reactions studied, but not for the (p, p') reactions studied. In fact, there seems to be a slight decrease of N_γ for increasing A for DR (p, p') reactions [cf. Ref. 16 for discussion of which (p, p') reactions are CN and which are DR]. The similarity of N_γ for all (p, p') reactions studied is very strong.

(c) N_γ is quite large for $^{51}V(p, \alpha)$ compared to ^{56}Fe and $^{57}Fe(p, \alpha)$. Possible explanations for this are odd-even effects and the target-spin–residual-nucleus-spin argument discussed in remark (5) of the last section. For $^{51}V(p, \alpha)$, the target-nucleus spin is $\frac{7}{2}$ while the residual-nucleus spin is 0, which will tend to raise $\bar{I}$, but not very much according to Fig. 9, part (b). The difference between N_γ for the $^{51}V(p, \alpha)$ and $Fe(p, \alpha)$ reactions is larger than any of the other odd-even effects.

In order to further investigate the dependence of N_γ on the average excess angular momentum of the residual nucleus, $|\bar{I} - I_R|$, N_γ vs $|\bar{I} - I_R|$ is plotted in Fig. 10, part (a), for 17 reactions for which $\bar{I}$ is calculable [assuming a CN reaction mechanism except for (d, p) reactions] for $E^* = 6.65$ MeV. The data points enclosed in parentheses are for reactions forming odd-A nuclei with excited states below 380 keV excitation (the measured N_γ is expected to be low for these points due to undetected γ rays). The pattern of the data points indicates that N_γ increases with $|\bar{I} - I_R|$ for $|\bar{I} - I_R|$ greater than 2 or 3, with N_γ somewhat above 3.0 for all $|\bar{I} - I_R|$ less than 2 or 3. A plot of neutron capture N_γ's (obtained from Refs. 3 and 4) vs $|\bar{I} - I_R|$, shown in Fig. 10, part (b), shows a similar behavior. The larger spread in data points may be attributed to the different residual-nucleus excitations—the N_γ measurements in Refs. 3 and 4 were made for $E^* = B_n$, the neutron binding energy for the product nucleus, which varies from 5 to 10.2 MeV and averages 7 MeV for the reported cases. Thus the plot in Fig. 10, part (b), superimposes E^* dependences on $|\bar{I} - I_R|$ dependences.

It may be noted that there is some evidence [Fig. 10, part (a)] that N_γ is larger (by about 0.5 γ rays) for (α, p) reactions than for the other reactions, even for the same $I - I_R$. Possibly the reaction mechanism is not all normal CN [recall the re-

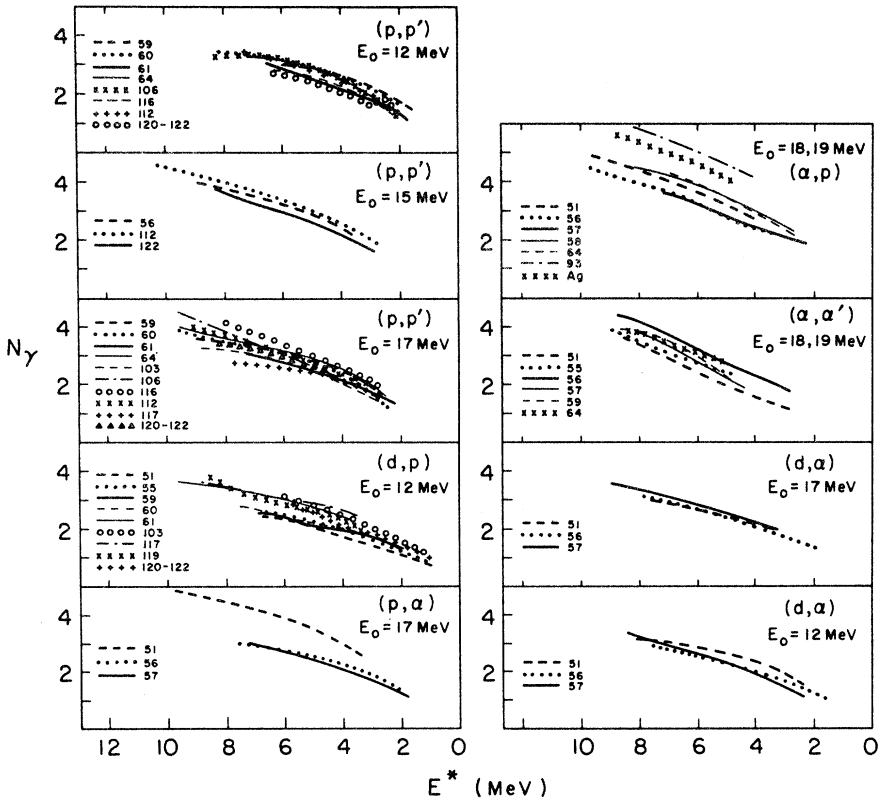

FIG. 5. Comparisons of N_γ for the same reactions on different targets. Different numbers indicate different target masses. (There is only one element for each target mass as indicated in the abstract.)

mark made earlier in this section on the anomalous dependence of the level-density parameter a on bombarding energy for (α, p) reactions[19]] which could make the calculations of $f(I)$ incorrect. Also, it would be more correct to say that N_γ depends on $f(I)$ and I_R than to say it depends on $|\bar{I} - I_R|$. It is not understood why N_γ should be larger for (α, p) reactions for the same $|\bar{I} - I_R|$.

Part (c) of Fig. 10 shows N_γ vs $|\bar{I} - I_R|$ for both the neutron-capture N_γ's and the results from this work. Also shown are calculated N_γ's for $|\bar{I} - I_R| = 2, 3$, and 4 obtained from Ref. 9. The similarity of the behavior of N_γ vs $|\bar{I} - I_R|$ for the three different sets of data gives additional confidence in the reliability of the method used in this work to determine N_γ, and suggests a possible technique for measuring the level-density spin-cutoff parameter σ.

The data points in Fig. 10 are too few and too scattered to say any more about σ than this: The theoretical σ's (those proposed by Gilbert and Cameron,[20] discussed in Appendix I) used to calculate the $\bar{I}$'s for the CN reactions are not inconsistent with the results in Fig. 10. However, if N_γ were measured for a large number of cases for which $\bar{I}$ is known or reliably calculable (with-

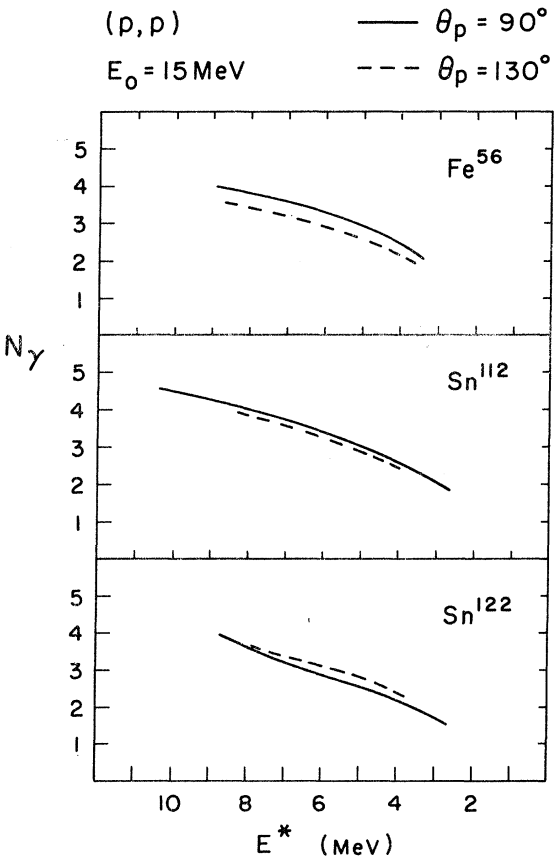

FIG. 6. Comparisons of N_γ for different charged-particle detection angles (90 and 130°) for (p, p') reactions with 15-MeV bombarding energy.

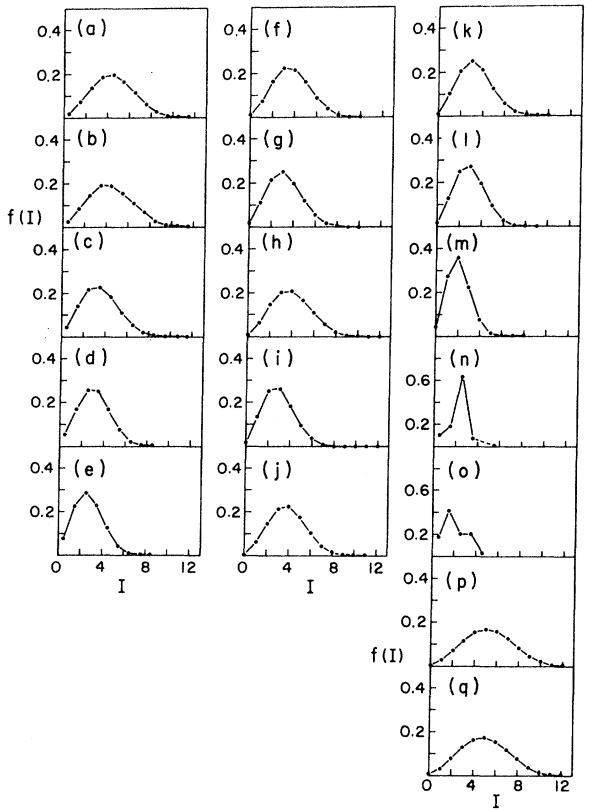

FIG. 7. (a)–(q) Calculated spin distributions. E is the bombarding energy, E^* is the residual-nucleus excitation energy, I is the residual-nucleus spin, and σ is the level-density spin-cutoff parameter for the residual nucleus.

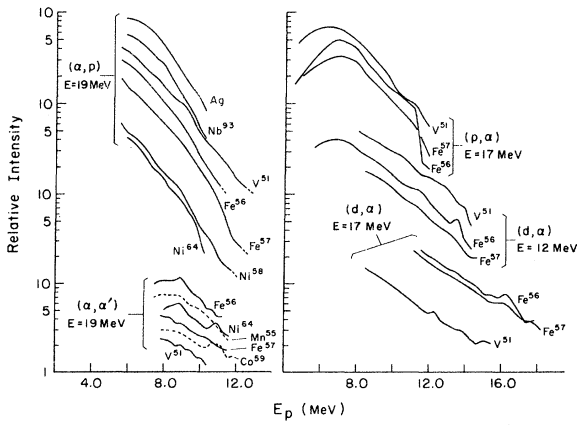

FIG. 8. Emitted charged-particle energy spectra. The shapes of the (α, p), (p, α), and (d, α) spectra are characteristic of CN reactions.

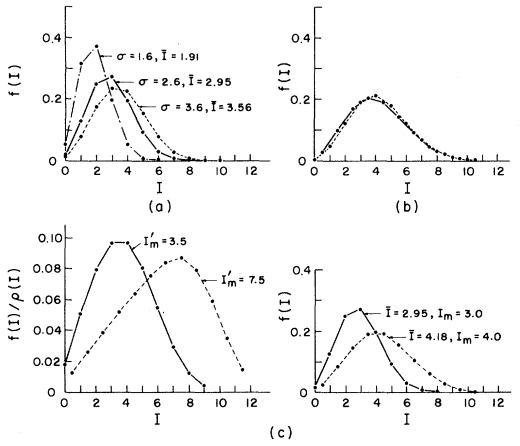

FIG. 9. (a) Effect of varying level-density spin-cutoff σ on residual-nucleus-spin distribution $f(I)$: ^{58}Ni(p,p'), $E_0 = 17.0$ MeV, $E^* = 7.5$. (b) Effect of target spin I_T on $f(I)$: ^{59}Co(α,p), $E_0 = 18.0$ MeV, $E^* = 8.0$, $\sigma = 3.0$. The symbols are as follows: —, $I_T = 0$ ($\bar{I} = 409$); – – –, $I_T = \frac{7}{2}$ ($\bar{I} = 4.24$). (c) Effect of spin part of level density $\rho(I)$ on $f(I)$: —, ^{58}Ni(p,p'), $E_0 = 17.0$ MeV, $E^* = 7.5$ MeV, $\sigma = 2.6$; – – –, ^{56}Fe(α,p), $E_0 = 18.0$ MeV, $E^* = 8.45$ MeV, $\sigma = 3.2$.

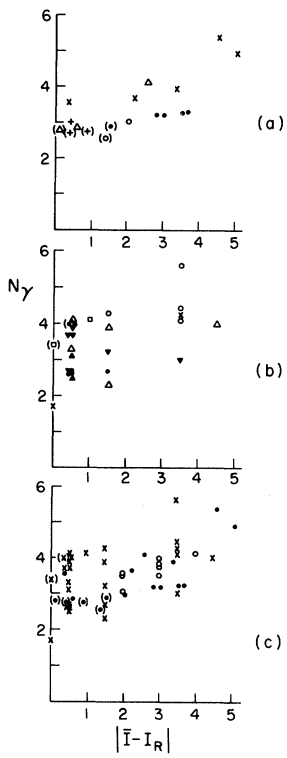

FIG. 10. N_γ vs average excess angular momentum $|\bar{I} - I_R|$ of residual nuclei: for (a) reactions investigated in this work [$E^* = 6.65$ MeV; ●, (p,p'), 17 MeV; △, (p,α), 17 MeV; +, (d,α), 12 MeV; ○, (d,p), 12 MeV; ×, (α,p), 19 MeV], (b) for neutron-capture cases (Refs. 3 and 4) [odd-odd product (▼, $B_m \leq 6.5$ MeV; ●, 6.5 MeV $< B_m <$ 8 MeV; ▲, $B_m \geq 8$ MeV), odd-A product (□, $B_m \leq 6.5$ MeV; ×, 6.5 MeV $< B_m <$ 8 MeV; +, $B_m \geq 8$ MeV), even-even product (▽, $B_m \leq 6.5$ MeV; ○, 6.5 MeV $< B_m <$ 8 MeV; △, $B_m \geq 8$ MeV), and (c) for cases (●, this work; ×, neutron-capture results; ○, calculated) plotted in (a) and (b) and for calculated cases (Ref. 9). Data points enclosed in parentheses in part (a) are for cases where complications from low-energy γ rays are expected (which would lower measured N_γ). Data points enclosed in parentheses in part (b) are for cases where low-energy isomeric states are present in the product nuclei—for these cases I_R means the isomeric state spin instead for the ground-state spin if the isomeric-state spin is closer to $\bar{I}$.

out using σ) for the same excitation energy, then the locus of known N_γ vs $|\bar{I} - I_R|$ points (an N-I diagram) could be used to relate N_γ to $\bar{I}$ (and hence, σ, for CN reactions) for cases where N_γ is known but $\bar{I}$ is not. Of course, such an N-I diagram would not be a line or curve but a band of data points, since the dependence of N_γ on $|\bar{I} - I_R|$ would be superimposed on the peculiarities of the lower excitation energy level schemes of the different residual nuclei, and since it is more correct to say that N_γ depends on $f(I)$ than to say that N_γ depends on $\bar{I}$.

V. CONCLUSIONS

The important results are the (expected) increase of N_γ with E^*, the fact that N_γ is considerably larger for (α,p) than for (d,p) reactions [expected because of the larger angular momentum transfer which, regardless of reaction mechanism, would tend to result in higher $\bar{I}$'s for (α,p) reactions], the increase of N_γ with target-nucleus mass A observed in (d,p) and (α,p) reactions, and the similarity of N_γ for all the (p,p') reactions studied. It is interesting that the size of the difference in N_γ for high angular momentum transfer reactions [namely, (α,p) and (α,α') reactions] and lower angular momentum transfer reactions can be qualitatively explained in terms of spin distributions calculated assuming a CN reaction mechanism, even for reactions which may be DR [e.g. (α,α') and the known[16] DR (p,p') reactions].

In comparing N_γ vs the residual-nucleus excess angular momentum $|\bar{I} - I_R|$ [calculated assuming a CN reaction mechanism except for (d,p) reactions], it appears that N_γ increases for $|\bar{I} - I_R|$ greater than 2 or 3 units, and there is some indication that N_γ is larger (by about 0.5 γ rays at $E^* = 6.65$ MeV) for (α,p) reactions than for other reactions at the same $|\bar{I} - I_R|$. The latter point is not well understood.

The values of N_γ for similar excitation energies for the reactions studied in this work and for neutron capture[3,4] are similar (cf. Fig. 3). Comparison of the measured N_γ vs calculated $|\bar{I} - I_R|$ from this work with that from neutron-capture work indicates that the theoretical spin cutoff parameters used to calculate $\bar{I}$ (for the CN reactions) are reasonable, and suggests a possible technique to measure these parameters (or, at least, the $\bar{I}$'s).

APPENDIX: CALCULATION OF SPIN DISTRIBUTIONS OF RESIDUAL NUCLEI

(d,p) Reactions

From shell-model and stripping reaction theory, it is possible to calculate the strength with which single-particle states of each angular momentum are populated by (d, p) reactions. The differential cross section for (d, p) reactions populating a single-particle state with quantum numbers n, l, and j is given by[21,22]

$$\left(\frac{d\sigma}{d\Omega}\right)_{nlj} = 1.5\left(\frac{2J+1}{2J_T+1}\right) S_{nlj}\,\sigma_{\mathrm{JULIE}}(nlj)\,, \tag{A1}$$

where n is the radial quantum number (related to the number of nodes in the radial wave function of the single-particle state), l and j are the orbital and total angular momentum quantum numbers of the single-particle state, $d\Omega$ is the solid-angle element into which the proton is emitted, J_T is the spin of the target nucleus, $\sigma_{\mathrm{JULIE}}(nlj)$ is the cross section calculated by the DWBA program JULIE,[22] and S_{nlj} is the spectroscopic strength which contains the nuclear-structure information and represents how similar the state of the residual nucleus is to a single-particle state (nlj) coupled to the ground state of the target nucleus.

For even-even target nuclei ($J_T = 0$), the spin distribution of the residual nucleus can be obtained directly from the differential cross sections for populating single-particle states of different J's. For odd-A target nuclei, angular momentum coupling of the single-particle states with the target-nucleus ground state must be taken into account. In this work, spin distributions were calculated for ^{56}Fe(d, p) reactions ($J_T = 0$) and ^{119}Sn(d, p) reactions ($J_T = \frac{1}{2}$). For $J_T = \frac{1}{2}$, the residual-nucleus spin is $I = J \pm \frac{1}{2}$ (where J is the spin of the single-particle state populated by the reaction), so that the spin distribution is nearly the same as for $J_T = 0$.

For higher excitation energies, the spectroscopic strength S_{nlj} can be estimated by assuming that it is a function of excitation energy centered on the excitation energy E^*_{nlj} corresponding to excitation of the single-particle state nlj and that the function falls to one half its maximum value for excitation $E^* = E^*_{nlj} \pm W(E^*_{nlj})$ where $W(E^*_{nlj})$ is the imaginary part of the optical-model potential used to calculate scattering and reaction cross sections.[23] $W(E^*_{nlj})$ can be estimated from[23]

$$W(E^*) \simeq \tfrac{1}{3}E^* \tag{A2}$$

and E^*_{nlj} is given by[23]

$$E^*_{nlj} = \epsilon_{nlj} + S_n\,, \tag{A3}$$

where S_n is the neutron binding energy (of the residual nucleus in its ground state) and ϵ_{nlj} is the single-particle energy, obtained from Ref. 24.

In this work, a Gaussian distribution centered on E^*_{nlj} with a full width at half maximum of $2W(E^*_{nlj})$, normalized to have an area of unity was assumed for $S_{nlj}(E^*)$:

$$S_{nlj}(E^*) = \frac{1}{1.44\sqrt{\pi}\,W_{nlj}} \exp[(E^* - E^*_{nlj})^2/1.44W^2(E^*_{nlj})]. \tag{A4}$$

In practice, only those states for which the difference between E^* and E^*_{nlj} is less than $2W(E^*_{nlj})$ need be considered.

In this work, spin distributions were calculated for ^{56}Fe(d, p) and ^{119}Sn(d, p) with excitation energies of 6.4 and 6.9 MeV, respectively, and with a bombarding energy of 12 MeV. The spin distributions were obtained using Eq. (A1). Since only single-particle states in the next major shell [$2d_{5/2}$, $1g_{7/2}$, $3s_{1/2}$, $2d_{3/2}$, and $1h_{11/2}$ for ^{56}Fe(d, p); $1h_{9/2}$, $2f_{7/2}$, $3p_{3/2}$, $2f_{5/2}$, and $3p_{1/2}$ for ^{119}Sn(d, p)] are important, only one single-particle state corresponds to each angular momentum J. Thus, the (unnormalized) spin distribution for each reaction is just the set of differential cross sections for populating the single-particle states of each J.

The optical-model parameters used in code JULIE were Perey parameters for protons and Perey B parameters for deuterons.[25-27]

CN Reactions

If the reaction mechanism for $A(a, b)B$ is compound nucleus the reaction proceeds as

$$a + A \rightarrow C$$
$$C \rightarrow B + b.$$

In order to calculate the spin distribution of the residual nucleus B one first calculates the spin distribution of the intermediate compound nucleus C. The cross section for forming C with spin I_c is[13-15]

$$\sigma_c = \pi\lambda^2 \frac{(2I_c+1)}{(2s+1)(2I_T+1)}\, T(I_T, E_0, I_c), \tag{A5}$$

where I_T is the spin of the target nucleus, s and E_0 are the spin and energy of the incident particle, $\lambda\!\!\!^{-}$ is the reduced wavelength of the incident particle, and

$$T(i,E,j)=\sum_{S=|i-s|}^{i+s}\sum_{l=|j-s|}^{j+s}T_l(E). \tag{A6}$$

In Eq. (A6), $T_l(E)$ is the transmission coefficient (barrier penetrability) for a particle with energy E, spin s, and angular momentum l—the type of particle and the nucleus it is incident on must also be defined, of course. In Eq. (A5), $T(I_T,E_0,I_c)$ is a double sum over transmission coefficients for the particle incident on the target nucleus. The limits of the double sum can be understood in terms of angular momentum selection rules, since

$$\vec{I}_c=\vec{I}_T+\vec{s}+\vec{l}\ . \tag{A7}$$

There are $(2s+1)(2I_T+1)$ terms, each a transmission coefficient, in the double sum in $T(I_T,E_0,I_c)$. For I_T and s equal to zero, $T(I_T,E_0,I_C)$ is just $T_{I_c}(E_0)$ and σ_c is $\pi\lambda\!\!\!^{-2}(2I_c+1)T_{I_c}(E_0)$. The effect of I_T and s on σ_c is noticeable but small.

The next step in calculating the spin distribution of the residual nucleus B is to calculate the relative probability that a state of spin I_c in intermediate compound nucleus C will decay to a state of spin I_B in B by emission of an appropriate particle with energy E_1. According to statistical theory the relative probability for the decay is proportional[13,14,28] to $\rho(E_B,I_B)T(I_B,E_1,I_c)$ where $\rho(E_B,I_B)$ is the level density[20] (per unit excitation energy) of the residual nucleus at excitation energy E_B, and $T(I_B,E_1,I_c)$ is a double sum over the transmission coefficients for the emitted particle b incident on the residual nucleus B with the energy E_1. There are $(2s_1+1)(2I_B+1)$ terms, each a transmission coefficient, in $T(I_B,E_1,I_c)$, where s_1 is the spin of the emitted particle b.

An unnormalized spin distribution of B is given by

$$P_B(I_B)=\sum_{I_c}\sigma_c(I_T,E_0,I_c)\rho(E_B,I_B)T(I_B,E_1,I_c). \tag{A8}$$

The $\pi\lambda\!\!\!^{-2}$ and $\rho(E_B)$ can be factored out of the above equation [$\rho(E_B,I_B)=\rho(E_B)\rho(I_B)$ as discussed in Ref. 20], yielding an unnormalized spin distribution for B given by

$$f(I_B)=\sum_{I_c}\frac{(2I_c+1)}{(2s+1)(2I_T+1)}\,T(I_T,E_0,I_c)\times\rho(I_B)T(I_B,E_1,I_c)\ , \tag{A9}$$

where $\rho(I_B)$ is[20]

$$(2I_B+1)\exp[-(I_B+\tfrac{1}{2})^2/2\sigma^2] \tag{A10}$$

as discussed in Ref. 20. In Eq. (A10), σ is the level-density spin cutoff parameter. In this work, the Gilbert and Cameron values[20] of σ were used. As discussed in Sec. V of this paper, $f(I_B)$ is strongly dependent on $\rho(I_B)$—it is proportional to it.

The transmission coefficients used in the spin-distribution calculations were obtained using the code SINGLE.[29] Perey and Perey B parameters[25-27] (which are generated by the code SINGLE) were used for protons and deuterons, respectively. The optical-model parameters for α particles were obtained from the work by McFadden and Satchler.[30] The McFadden and Satchler parameters (which use volume absorption) are for an α energy of 24.7 MeV, so the volume absorption W was assumed to be proportional to the excitation energy of the product nucleus formed by α capture.[23]

---

*Work supported by the National Science Foundation.

†Present address: Air Force Weapons Laboratory, Kirtland Air Force Base, New Mexico 87117.

[1]J. H. Degnan, B. L. Cohen, R. C. Petty, C. L. Fink, G. R. Rao, and R. Balasubramanian, Phys. Rev. C 5, 836 (1972).

[2]J. H. Degnan, B. L. Cohen, G. R. Rao, and K. C. Chan, Phys. Rev. C 6, 248 (1972).

[3]C. O. Muehlhause, Phys. Rev. 79, 277 (1950).

[4]J. E. Draper and T. E. Springer, Nucl. Phys. 16, 27 (1960).

[5]F. Pleasonton, R. L. Ferguson, and H. W. Schmitt, Phys. Rev. C 6, 1023 (1972).

[6]V. V. Verbinski, H. Weber, and R. E. Sund, Phys. Rev. C 7, 1173 (1973).

[7]J. F. Mollenauer, Phys. Rev. 127, 867 (1972).

[8]L. V. Groshev, V. N. Lutsenko, A. M. Demidov, and V. I. Pelekov, *Atlas of Gamma Ray Spectra from Radiative Capture of Thermal Neutrons* (Pergamon, N.Y., 1959) translated from Russian by J. B. Sykes.

[9]C. Coceva, F. Corvi, and P. Giacobbe, Nucl. Phys. A117, 586 (1968).

[10]A. Stolovy, A. I. Namenson, J. C. Ritter, T. F. Godlove, and G. L. Smith, Phys. Rev. C 5, 2030 (1972).

[11]J. R. Huizenga and R. Vandenbosch, Phys. Rev. 120, 1305 (1960); *ibid.* 120, 1313 (1960).

[12]Care must be taken to distinguish between the average angular momentum of states *excited by a reaction* (in a given energy interval) and the average angular momentum of the states *available for excitation* (by any process, in the same excitation energy interval). The average angular momentum $\bar{I}$ of the residual nucleus is the former, not the latter.

[13]J. H. Degnan, Ph.D. thesis, University of Pittsburgh, 1973 (unpublished).

[14]C. L. Fink and B. L. Cohen, Phys. Rev. C 6, 1973

(1972).
[15]J. R. Grover, Phys. Rev. 123, 267 (1961); 127, 2142 (1962); J. R. Grover and R. J. Nagle, *ibid.* 134, B1248 (1964); J. R. Grover and J. Gilat, *ibid.* 157, 802 (1967); 157, 814 (1967).
[16]G. R. Rao, R. Balasubramanian, B. L. Cohen, C. L. Fink, and J. H. Degnan, Phys. Rev. C 4, 1855 (1971).
[17]N. O. Lassen and V. A. Sidrov, Nucl. Phys. 19, 579 (1960).
[18]C. C. Lu, J. R. Huizenga, C. J. Stephen, and A. J. Gorski, Nucl. Phys. A164, 225 (1971).
[19]W. Swenson and N. Cindro, Phys. Rev. 123, 910 (1961).
[20]A. Gilbert and A. G. W. Cameron, Can. J. Phys. 43, 1446 (1965).
[21]R. H. Bassel, R. M. Drisko, and G. R. Satchler, Oak Ridge National Laboratory Report No. 3240, 1962 (unpublished).
[22]R. H. Bassel, R. M. Drisko, and G. R. Satchler, Oak Ridge National Laboratory Memorandum on code JULIE, 1966 (unpublished); code JULIE was kindly provided by R. M. Drisko.
[23]B. L. Cohen, *Concepts of Nuclear Physics* (McGraw-Hill, New York, 1971).
[24]B. L. Cohen, Am. J. Phys. 33, 1011 (1965).
[25]F. G. Perey, Phys. Rev. 131, 745 (1963).
[26]C. M. Perey and F. G. Perey, Phys. Rev. 132, 755 (1963).
[27]D. R. Winner and R. M. Drisko, University of Pittsburgh Technical Report, 1965 (unpublished).
[28]T. Darrah Thomas, Nucl. Phys. 53, 558 (1964); T. Ericson, Advan. Phys. 63, 479 (1960).
[29]SINGLE is the University of Pittsburgh version of F. G. Perey's optical-model code JIB.
[30]L. McFadden and G. R. Satchler, Nucl. Phys. 84, 177 (1966).